

ORIGINAL ARTICLE

Chondroinduction from Naturally Derived Cartilage Matrix: A Comparison Between Devitalized and Decellularized Cartilage Encapsulated in Hydrogel Pastes

Emily C. Beck, PhD,¹ Marilyn Barragan,² Tony B. Libeer,³ Sarah L. Kieweg, PhD,⁴ Gabriel L. Converse, PhD,⁵ Richard A. Hopkins, MD,⁵ Cory J. Berkland, PhD,^{3,6} and Michael S. Detamore, PhD⁴

Hydrogel precursors are liquid solutions that are prone to leaking after surgical placement. This problem was overcome by incorporating either decellularized cartilage (DCC) or devitalized cartilage (DVC) microparticles into traditional photocrosslinkable hydrogel precursors in an effort to achieve a paste-like hydrogel precursor. DCC and DVC were selected specifically for their potential to induce chondrogenesis of stem cells, given that materials that are chondroinductive on their own without growth factors are a revolutionary goal in orthopedic medicine. We hypothesized that DVC, lacking the additional chemical processing steps in DCC to remove cell content, would lead to a more chondroinductive hydrogel with rat bone marrow-derived mesenchymal stem cells. Hydrogels composed of methacrylated hyaluronic acid (MeHA) and either DCC or DVC microparticles were tested with and without exposure to transforming growth factor (TGF)- β_3 over a 6 week culture period, where swelling, mechanical analysis, and gene expression were observed. For collagen II, Sox-9, and aggrecan expression, MeHA precursors containing DVC consistently outperformed the DCC-containing groups, even when the DCC groups were exposed to TGF- β_3 . DVC consistently outperformed all TGF- β_3 -exposed groups in aggrecan and collagen II gene expression as well. In addition, when the same concentrations of MeHA with DCC or DVC microparticles were evaluated for yield stress, the yield stress with the DVC microparticles was 2.7 times greater. Furthermore, the only MeHA-containing group that exhibited shape retention was the group containing DVC microparticles. DVC appeared to be superior to DCC in both chondroinductivity and rheological performance of hydrogel precursors, and therefore DVC microparticles may hold translational potential for cartilage regeneration.

Introduction

TRADITIONAL HYDROGELS are a promising class of regenerative materials for cartilage regeneration, but they lack the ability to be molded into a defect site by a surgeon because hydrogel precursors are liquid solutions that are prone to leaking after placement.^{1,2} To overcome this drawback, we recently introduced a method to achieve paste-like hydrogel precursor solutions by combining hyaluronic acid nanoparticles with traditional crosslinked hyaluronic acid hydrogels, where the paste-like behavior was induced by the presence of the hyaluronic acid nanoparticles.³ These hyaluronic acid formulations were then crosslinked to form a

rigid traditional hydrogel structure. In an effort to introduce bioactivity to the material, in this study we substituted the hyaluronic acid nanoparticles for particles made from naturally derived cartilage extracellular matrix (ECM).

ECM-based materials are attractive for regenerative medicine because of their ability to potentially aid in stem cell recruitment, infiltration, and differentiation without supplementing with additional biological factors.^{4–6} These ECM materials can be obtained from cell-derived matrices secreted during *in vitro* culture or from native tissue,^{4,7–11} and they have either been decellularized to remove cellular components and nucleic acids or they have been devitalized to kill but not necessarily remove cells within the matrix.¹²

¹Department of Surgery, University of Kansas Medical Center, Kansas City, Kansas.

Departments of ²Molecular Biosciences, ³Chemical and Petroleum Engineering, and ⁴Mechanical Engineering, University of Kansas, Lawrence, Kansas.

⁵Cardiac Surgery Research Laboratory, Children's Mercy Hospital, Kansas City, Missouri.

⁶Department of Pharmaceutical Chemistry, University of Kansas, Lawrence, Kansas.

We and other groups have already established that cartilage matrix has chondroinductive potential,^{7,13–17} and we recently were the first to compare the chondroinductive potential of two different types of cartilage matrix in pellet culture: devitalized cartilage (DVC), where the matrix was exposed to a freeze/thaw process to devitalize the living chondrocytes within the matrix, and decellularized cartilage (DCC), in which the cells were not only devitalized but also removed from the matrix entirely.¹⁷

In the pellet culture study, we observed that rat bone marrow stem cells (rBMSCs) exposed to DCC outperformed those cells exposed to DVC or transforming growth factor- β_3 (TGF- β_3) in chondroinductivity.¹⁷ However, gene expression was only observed over a period of 7 days and was only monitored for cells in pellet culture and not within a 3D scaffold.

Although it is widely emphasized that for ECM-based tissues, in general, improper decellularization can result in detrimental inflammatory responses and hinder tissue regeneration,¹⁸ cartilage matrix is uniquely immunoprivileged, in part, because cartilage matrix is so dense that it protects chondrocytes from T and natural killer cells that are released in graft rejection.¹⁹ Regarding immune response of allogeneic cartilage matrix, the success of Zimmer's DeNovo[®] product supports the potential for DVC, as DeNovo relies on juvenile human cartilage donation with living chondrocytes and has no reports of allograft rejection or disease transmission.

In addition, DeNovo cartilage has been observed to create hyaline-like cartilage in goats, where no T-cell-mediated response was noted.²⁰ Therefore, for some cartilage tissue applications, this success with a technology that includes cells brings up the question of whether or not decellularization is even necessary. Although the goal of decellularization is to remove all of the cells without destroying the structure and composition of the ECM, all decellularization processes inevitably cause some disruption to the matrix architecture, orientation, and surface landscape,²¹ which may ultimately limit or hinder the chondroinductive potential of the matrix, especially if the decellularization removes or alters the bioactive molecules that are responsible for inducing chondrogenesis.

Therefore, because the long-term chondroinductive potential of DCC and DVC has yet to be explored, the objective of this work was to compare the chondroinductivity of DVC versus DCC in a "generic" hydrogel (i.e., a hydrogel not known for superior mechanical or chondroinductive performance) composed of methacrylated hyaluronic acid (MeHA) for 6 weeks *in vitro* to aid in determining whether one of these ECM-based materials may be superior for future cartilage tissue engineering applications. In addition, another objective was to observe how DVC and DCC affected the rheology of the hydrogel precursors. We hypothesized that a paste-like material composed of DVC would induce superior chondrogenesis compared with that of DCC and compared with hydrogels exposed to TGF- β_3 or the combination of DCC and TGF- β_3 over the 6-week period.

Materials and Methods

Synthesis and characterization of MeHA

MeHA was prepared by reacting hyaluronic acid (MW 1 MDa, Lifecore Biomedical, Chaska, MN) with 20-fold molar

excess glycidyl methacrylate (Sigma-Aldrich, St. Louis, MO) in the presence of triethylamine and tetrabutyl ammonium bromide (Sigma-Aldrich) in a 50:50 water:acetone mixture and stirring at 200 rpm for 12 days. MeHA was then dialyzed against deionized (DI) water for 2 days and then frozen at -80°C and lyophilized. The degree of methacrylation was determined using ^1H NMR (Avance AV-III 500; Bruker) by calculating the ratio of the relative peak area of methacrylate protons to methyl protons.²²

Tissue retrieval, devitalization, and decellularization

Ten porcine knees obtained from Berkshire hogs (castrated males that were ~ 7 –8 months old and 120 kg) were purchased from a local abattoir (Bichelmeyer Meats, Kansas City, KS). Articular cartilage from both the knee and hip joints was carefully removed and collected with a scalpel. The cartilage was rinsed twice in DI water and stored at -20°C . After freezing overnight, the cartilage was thawed and then coarsely cryoground with dry ice pellets using a cryogenic tissue grinder (BioSpec Products, Bartlesville, OK). The dry ice was allowed to sublime overnight in the freezer and at this point all of the cartilage was devitalized because of undergoing the freeze/thaw processes. Some of the DVC was saved for the study and the rest was processed to make DCC.

To decellularize the cartilage, the coarse ground cartilage was packed into dialysis tubing (3500 MWCO) and decellularized by an adapted version of our previously established method using osmotic shock, detergent, and enzymatic washes.²³ The packets were placed in a hypertonic salt solution (HSS) overnight at room temperature under gentle agitation (70 rpm). The packets were then subjected to 220 rpm agitation with two reciprocating washes, encompassing triton X-100 (0.01% v/v) followed by HSS, to permeabilize intact cellular membranes. The tissue was then treated overnight with benzonase (0.0625 KU/mL) at 37°C and then the tissue was treated with sodium-lauroylsarcosine (NLS, 1% v/v) overnight to further lyse cells and denature cellular proteins. After NLS exposure, the tissue was washed with ethanol (40% v/v) at 50 rpm and then was subjected to organic exchange resins to extract the organic solvents at 65 rpm. The tissue was then washed in saline-mannitol solution at 50 rpm followed by 2 h of rinsing with DI water at 220 rpm. The tissue was then removed from the packets and was then frozen and lyophilized.

Both the DVC and DCC were then further cryoground into a fine powder with a freezer-mill (SPEX SamplePrep, Metuchen, NJ) and then lyophilized. The DCC and DVC powders were filtered using a $45\text{ }\mu\text{m}$ mesh (ThermoFisher Scientific, Waltham, MA) to remove large particles and then frozen until use.

Scanning electron microscopy

DCC and DVC microparticles were sputter coated with gold and imaged with a Versa 3D Dual Beam (FEI, Hillsboro, OR) to observe their surface morphology and size.

rBMSC harvest and culture

rBMSCs were harvested from the femurs of three male Sprague-Dawley rats (200–250 g) following an approved IACUC protocol at the University of Kansas. The rBMSCs

were first harvested in minimum essential medium- α (MEM- α ; ThermoFisher) with 10% fetal bovine serum (FBS, MSC qualified, ThermoFisher) and 1% antibiotic-antimycotic (ThermoFisher) and then cultured in this medium for 1 week to ensure no mycotic contamination from harvesting. The rBMSCs were then cultured in MEM- α supplemented with 10% FBS and 1% penicillin/streptomycin (ThermoFisher) until the cells reached passage 4 for cell encapsulation into the hydrogels.

Description of experimental groups

The four formulations tested for the cell-based analyses using crosslinked hydrogels were 3% (by weight) MeHA, 3% MeHA + 5% DCC, 3% MeHA + 10% DCC, and 3% MeHA + 10% DVC. Because native ECM is incorporated into the pastes, acellular formulations of the same four groups were prepared and analyzed with the cellular groups to quantify the acellular biochemical content and to analyze the effect of cells encapsulated in the networks. The 3% concentration was chosen for MeHA as it was near the reconstitution limit of MeHA at its particular molecular weight. The 10% concentration was chosen for DCC and DVC because it was the percentage that yielded a moderate yield stress (e.g., 100 Pa) without affecting the ability to crosslink the paste when exposed to UV light as the particles are not transparent and concentrations more than 10% were difficult to crosslink.

Both the MeHA and MeHA + 10% DCC groups were tested with and without exposure to 10 ng/mL human TGF- β_3 (PeproTech, Inc., Rocky Hill, NJ). For the rheological testing before crosslinking, additional groups of 2.5% DCC, 5% DCC, and 10% DCC, all of which did not contain MeHA, were tested. DCC and DVC alone cannot be crosslinked into a hydrogel network, which is why these three DCC groups were only tested rheologically.

Preparation of hydrogel pastes, cell encapsulation, and hydrogel culture conditions

Hydrogel pastes were made first by measuring out the desired weight percentages of MeHA, DVC, or DCC into a mini-centrifuge tube. All materials for cellular analyses were then sterilized with ethylene oxide before use and were handled under sterile conditions thereafter. All gels were mixed in two stages (e.g., in photoinitiator solution overnight and then more photoinitiator or cell suspension on the day of testing) because some of the samples required mixing with cells and the time it took for MeHA to dissolve to ensure mixture homogeneity (i.e., overnight) was deemed too long for adequate cell survival. Therefore, cell mixtures were added the next day after the MeHA was given a chance to dissolve in half of the final solution.

For acellular rheological testing, sterile 0.01 M phosphate-buffered saline (PBS) containing 0.05% (w/v) Irgacure (I-2959) photoinitiator was added until the concentration of MeHA and DCC was twice the desired concentration. The samples were mixed, centrifuged, and placed in 4°C overnight to allow time for the MeHA to dissolve. Before testing, more photoinitiator solution was added until the desired concentration was reached and the samples were again mixed and centrifuged to remove air bubbles. For example, to make a 3% MeHA solution, 12 mg MeHA and 200 μ L photoinitiator solution were mixed and allowed to dissolve

overnight and then another 200 μ L photoinitiator solution was added to make the final concentration at 3% MeHA.

For cellular testing, the samples were mixed with 0.1% (w/v) Irgacure photoinitiator in PBS until the concentration of MeHA and DCC was twice the desired final concentration, and then the solutions were centrifuged and stored at 4°C overnight. Passage 4 rBMSCs were then suspended at 20 million cells/mL in incomplete chondrogenic medium consisting of high glucose DMEM (ThermoFisher) with 4.5 g/L D glucose supplemented with 10% FBS, 1% nonessential amino acids, 1% sodium pyruvate, 50 μ g/mL ascorbic acid, and 0.25 mg/mL penicillin/streptomycin. This cell solution was then added to the hydrogel paste solutions until the desired concentration of MeHA and DCC or DVC was reached and the final cell concentration and photoinitiator concentrations were 10 million cells/mL and 0.05%, respectively.

The solutions were then either tested rheologically or crosslinked with UV light and further characterized as solids. For gels undergoing crosslinking, hydrogel precursor pastes were loaded into 2 mm thick molds between glass slides and exposed to 312 nm UV light at 3.0 mW/cm² in a UV crosslinker (Spectrolinker XL-100; Spectronics Corporation, Westbury, NY) for 2.5 min on each side. Each gel was then cut using a 4 mm biopsy punch and placed in one well of a 24 well, nontissue culture-treated plate (Corning Incorporated, Corning, NY). Each gel was exposed to 1 mL of incomplete chondrogenic medium or 1 mL of complete chondrogenic medium, which consisted of incomplete chondrogenic medium plus 0.1 mg/mL dexamethasone and 10 ng/mL TGF- β_3 . The medium was replaced every other day throughout the 6 weeks of culture.

Rheological testing of hydrogel precursors

Before crosslinking the hydrogels, the precursor solutions were loaded into a 3 mL syringe and extruded onto a glass slide to macroscopically observe shape retention. The gels were extruded in a wavy line appearance to observe whether the formulations maintained their shape after crosslinking.

Using an AR-2000 rheometer (TA Instruments, New Castle, DE), the oscillatory shear stress of the precursor solutions ($n=5$) was measured over an oscillatory shear stress sweep of 1–600 Pa at 37°C, where the rheometer was equipped with a 20 mm diameter roughened plate and a roughened Peltier plate cover using a gap of 500 μ m. Frozen rBMSCs that were thawed and cultured to passage 4 were used to make cellular samples for rheological testing. The pastes were then created as previously mentioned for *in vitro* culture. The yield stress was interpolated from the oscillatory stress at which the storage (G') and loss (G'') modulus crossed.²⁴ An oscillatory shear stress sweep of 0.1–10 Pa was performed to assess the linear viscoelastic region of the solutions to determine the value of the storage modulus of each solution.

Mechanical testing of crosslinked hydrogels

The gels were allowed to swell to equilibrium for 1 day in either complete or incomplete chondrogenic medium and mechanical testing was performed at day 1 and 6 weeks. The geometric mean diameter of the gels was first determined using forceps and a stereomicroscope (20 \times magnification) and the height of each gel was measured directly with an

RSA-III dynamic mechanical analyzer (DMA; TA Instruments). The gels ($n=5$) were compressed on the DMA at a rate of 0.01 mm/s until mechanical failure and the modulus was calculated as the slope under the linear portion of the stress-strain curve (i.e., 0–10% strain).

Swelling degree and volume

To calculate the swelling degree, the swollen gels (swollen to equilibrium) were weighed after 1 day of swelling and then frozen and lyophilized. The dry weight was recorded after lyophilization and the swelling degree was calculated as the ratio of total wet mass to dry mass. The volume of the gels was recorded at day 1 and after 6 weeks of culture and was calculated from the diameter and height of the gels recorded during mechanical testing.

Biochemical content analysis

The biochemical content of the MeHA, DVC, and DCC and the biochemical content of the gels at day 1, 3 weeks, and 6 weeks were quantified ($n=5$). The gels were digested overnight in a 1.5 mL papain mixture consisting of 125 mg/mL papain from papaya latex, 5 mM *N*-acetyl cysteine, 5 mM EDTA, and 100 mM potassium PBS at 65°C. Because some gels remained undigested, the remaining undigested gels were removed from the digestion medium and redigested overnight at 37°C in 0.5 mL hyaluronidase (Sigma-Aldrich, at a concentration of 500 U/mL) in 0.1M PBS. Then 1 mL of fresh papain mixture was added to the hyaluronidase solution and allowed to digest overnight at 65°C. Both the first and second digestion solutions were stored at –20°C. Before biochemical analysis, all digestion solutions were allowed to thaw to room temperature and then vortexed and centrifuged at 10,000 rpm for 10 min to pellet fragments of polymers. The supernatant was then used to quantify biochemical contents.

According to manufacturer instructions and using a Cytation 5 Cell-Imaging Multi-Mode reader (Bio-Tek, Winooski, VT), DNA content was quantified with the PicoGreen assay (Molecular Probes, Eugene, OR), glycosaminoglycan (GAG) content was determined with the dimethylmethylene (DMMB) assay (Biocolor, Newtownabbey, Northern Ireland) using a chondroitin sulfate standard, and hydroxyproline content was quantified with a hydroxyproline detection kit (Sigma-Aldrich). To obtain the total biochemical content for each gel, each of the two digestions for each gel was quantified and later added together. GAG and hydroxyproline contents were not normalized to DNA and are rather shown in total because of the gels' inherent initial DNA contents.

Gene expression analysis

RNA was isolated and purified using Qiagen QIAshredders and an RNeasy Kit (Valencia, CA) according to the manufacturer's guidelines ($n=6$). A high capacity cDNA reverse transcription kit (Applied Biosystems, Foster City, CA) was used to convert isolated RNA into cDNA. Real-time quantitative polymerase chain reaction (PCR) was performed using a RealPlex MasterCycler (Eppendorf, Hauppauge, NY) and using TaqMan gene expression assays from Applied Biosystems for Sox-9 (Rn01751070_m1), aggrecan (Rn00573424_m1), collagens types I (Rn01463848_m1) and II (Rn01637087_m1),

and GAPDH (Rn01775763_g1). The $2^{-\Delta\Delta C_t}$ method was used to quantify relative expression levels for each gene, where the MeHA gels at day 1 were designated as the calibrator group and GAPDH expression was used as the endogenous control.²⁵

Last, RNA from DVC and DCC (i.e., no rBMSCs) was isolated, converted to DNA, and then PCR was performed with the same previously mentioned TaqMan assays, where it was confirmed that all gene expression observed in this study was due to rBMSCs.

Histological analysis

Gels at day 1 and cellular gels at 6 weeks were fixed in 10% formalin for 15 min and then embedded in optimal temperature cutting medium (TissueTek, Torrance, CA) overnight at 37°C, frozen at –20°C, and were sectioned at a thickness of 10 μ m using a cryostat (Microm HM-550 OMP, Vista, CA). The sections were stained with the standard hematoxylin and eosin stain, which stains the nuclei purple and the cytoplasm, connective tissues, and other extracellular substances red or pink. The sections were stained with the standard Safranin-O/ Fast Green stain, which stains negatively charged GAGs orange.

The sections were stained immunohistochemically using primary antibodies that target both rat and porcine tissues for collagen I (NB600408, 1:200 dilution; ThermoFisher), collagen II (ab34712, 1:200 dilution; Abcam), and aggrecan (MA3-16888, 1:100 dilution; ThermoFisher). Before primary antibody incubation, the slides were fixed in chilled acetone (–20°C), treated with proteinase K (Abcam), and exposed to 0.3% hydrogen peroxide (Abcam) to suppress endogenous peroxidase activity. Sections were blocked with serum according to the Vectastain ABC kit (Vector Laboratories, Burlingame, CA) following the manufacturer's instructions and then incubated with primary antibody. After incubation with the primary antibodies, the sections were exposed to biotinylated secondary antibodies (horse anti-rabbit or mouse) and ABC reagent according to the manufacturer's protocol.

The antibodies were observed using the ImmPact DAB peroxidase substrate (Vector), rinsed in DI water, counterstained with VECTOR hematoxylin QS stain, and then dehydrated and mounted. Negative controls consisted of substituting primary antibody exposure with exposure to a rabbit IgG isotype control (for collagens I and II, ab27478; Abcam) at an antibody concentration calculated to be the same used for the corresponding antibodies and omitting the primary antibody for aggrecan.

Statistical analysis

GraphPad Prism 6 statistical software (GraphPad Software, Inc., La Jolla, CA) was used to compare experimental groups using a one-factor ANOVA (for analyses with one time point) or a two-factor ANOVA (for analyses with two or more time points) followed by a Sidak's *post hoc* test (for two-way ANOVAs with two time points only) or a Tukey's *post hoc* test (for all other ANOVAs), where $p \leq 0.05$ was considered significant. In addition, standard box plots were constructed to eliminate outliers. All quantitative results are reported as mean \pm standard deviation within text or as mean + standard deviation within figures.

Results

Characterization of MeHA, DVC, and DCC microparticles

Analyzing the ratio of the relative peak area of methacrylate protons to methyl protons of MeHA revealed that the MeHA had a 1.2% degree of methacrylation and the DNA and hydroxyproline contents were determined to be 9.2 ± 3.7 ng DNA/mg MeHA and 0.74 ± 0.14 μ g hydroxyproline/mg MeHA, respectively (Fig. 1A–C). Because the GAG assay only detects sulfated GAGs and hyaluronic acid is a non-sulfated GAG, the GAG content of MeHA was not detected. The DNA, GAG, and hydroxyproline contents of DVC were determined to be 1151 ± 51 ng DNA/mg dry DVC, 252 ± 16 μ g GAG/mg dry DVC, and 56.1 ± 3.9 μ g hydroxyproline/mg dry DVC, respectively (Fig. 1A–C).

After decellularization and cryogrinding to create DCC powder, there was a 44% reduction in DNA, a 23% reduction in GAG, and a 23% reduction in hydroxyproline ($p < 0.05$) (Fig. 1A–C). In prior work, it was established that

no significant reduction in biochemical content was observed between native cartilage and cartilage that was cryoground,¹⁷ so the prior mentioned reductions are in reference to DVC powder.

Scanning electron microscope (SEM) imaging revealed that DVC and DCC microparticles were ~ 45 μ m in diameter or smaller and were noted to be heterogeneous in size and morphology (Fig. 1D). The DCC microparticles were observed to have smoother surfaces overall in comparison with the DVC microparticles (Fig. 1D). Under higher magnification, observing the surface morphology revealed a grain-like appearance to the surface of the DCC microparticles that was not observed on the DVC microparticles (Fig. 1D).

Macroscopic observation and rheological testing of hydrogel precursor pastes

Macroscopic observation of hydrogel precursor formulations revealed non-Newtonian and paste-like behavior in

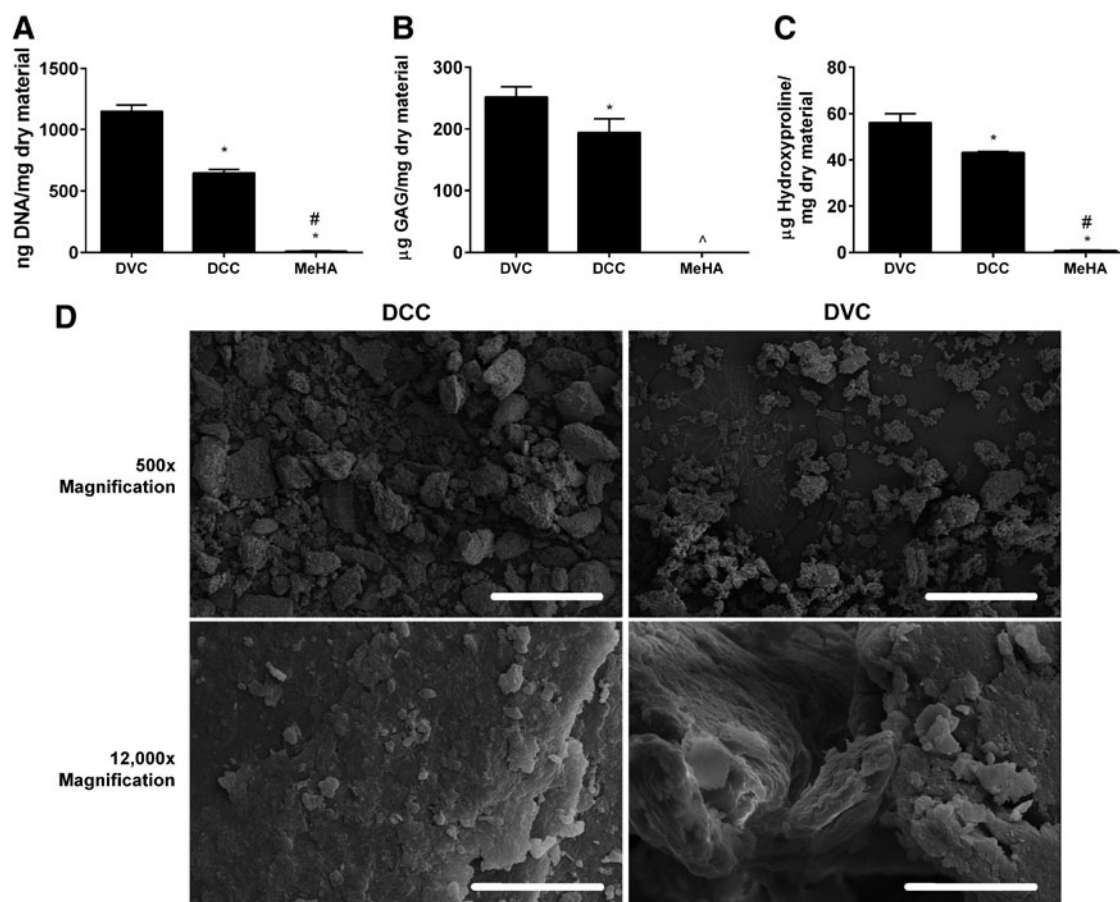


FIG. 1. Biochemical contents and SEM images of hydrogel paste components. (A) PicoGreen content, (B) GAG content, and (C) Hydroxyproline content of DVC, DCC, and MeHA. After decellularization, there was a 44% reduction in DNA, a 23% reduction in GAG, and a 23% reduction in hydroxyproline content. Data are reported as mean + standard deviation ($n = 5$); ^below detectable limit; *significantly different from DVC ($p < 0.05$); #significantly different from DCC ($p < 0.05$). (D) SEM images of DCC and DVC microparticles under 500 \times and 12,000 \times magnifications. Under 500 \times magnification, the DCC microparticles were noted to have more smooth surfaces overall than the DVC microparticles, and under 12,000 \times magnification, the surfaces of the DCC microparticles were noted to have a grain-like appearance that was nonexistent in the DVC microparticles. Scale bars for the 500 \times and 12,000 \times magnifications are 100 and 5 μ m, respectively. DCC, decellularized cartilage; DVC, devitalized cartilage; GAG, glycosaminoglycan; SEM, scanning electron microscope.

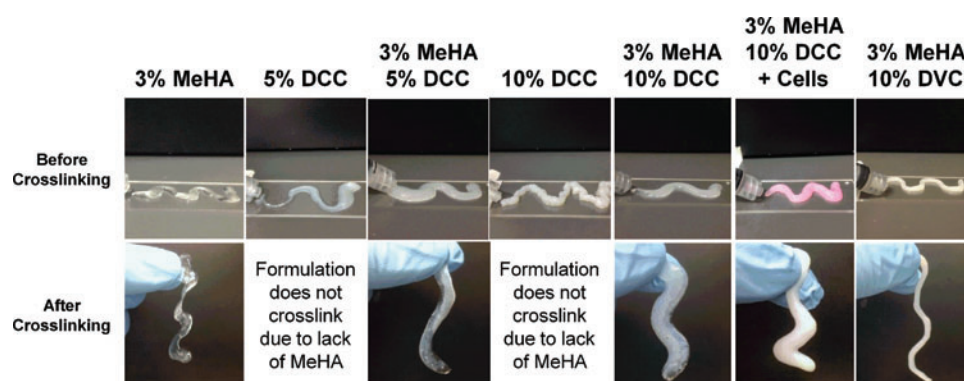


FIG. 2. Macroscopic rheological evaluation of hydrogel precursors before and after crosslinking. All formulations were acellular unless noted. Non-Newtonian behavior was observed in solutions containing at least 5% DCC, whereas shape retention (indicated by the solution retaining extrusion orifice diameter) was only noted in 10% DCC and 3% MeHA + 10% DVC acellular formulations. All formulations containing MeHA retained their shape after crosslinking. Color images available online at www.liebertpub.com/tea

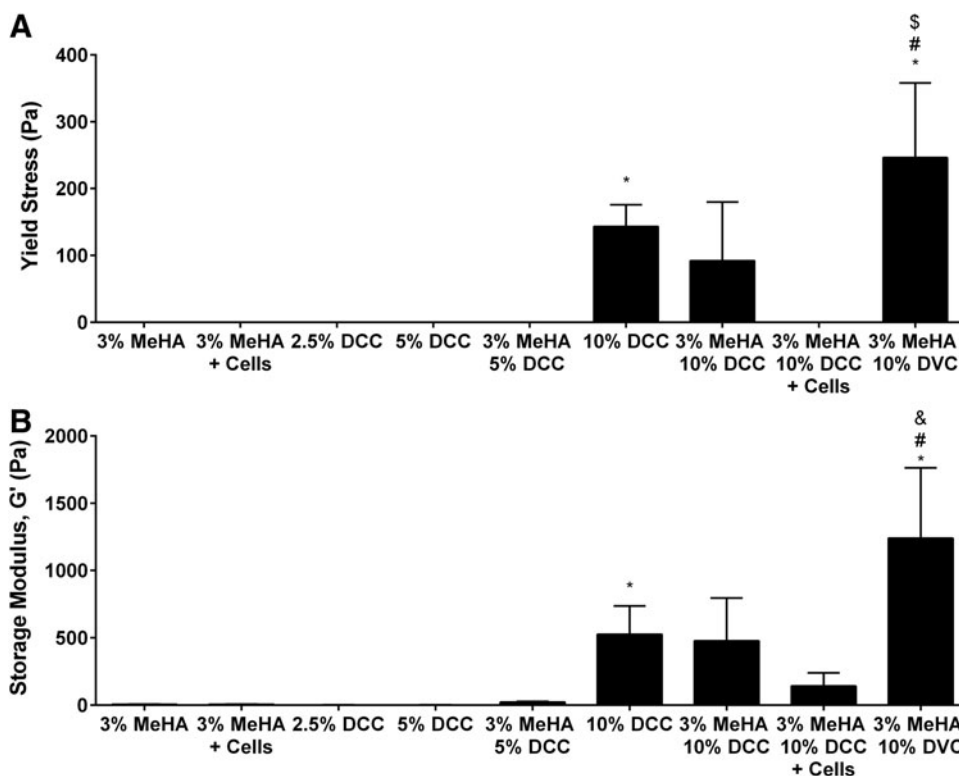
precursors containing at least 5% DCC (Fig. 2). Shape retention after extrusion through a 3 mL syringe, which was indicated by the fluid retaining the diameter of the syringe orifice after extrusion and after crosslinking, was noted in the 10% DCC and MeHA + DVC acellular groups (Fig. 2). The remaining solutions spread out to two to three times the diameter of the syringe orifice. All formulations containing MeHA were able to be crosslinked to maintain extrusion shape.

Solutions exhibiting a measurable yield stress were the 10% DCC, MeHA + 10% DCC, and MeHA + DVC formulations (Fig. 3A). The 10% DCC had a yield stress of 143 ± 33 Pa, whereas adding MeHA to 10% DCC reduced

the yield stress to 92 ± 88 Pa, although the reduction was not significant. The yield stress of the MeHA + DVC group was 2.7 and 1.7 times greater than that of the MeHA + 10% DCC and 10% DCC groups, respectively ($p < 0.05$) (Fig. 3A).

All of the groups exhibited viscoelastic behavior, as indicated by a measurable storage modulus. However, the storage modulus of the MeHA + DVC group was significantly higher than all of the other groups at 1240 ± 520 Pa, which was 58, 2.4, 2.6, and 8.8 times higher than the MeHA + 5% DCC, 10% DCC, MeHA + 10% DCC, and the cellular MeHA + 10% DCC cellular groups, respectively, which were the groups that had a storage modulus greater than 20 Pa ($p < 0.05$) (Fig. 3B).

FIG. 3. Yield stress (A) and storage modulus (B) of hydrogel precursor solutions. Only the 10% DCC, 3% MeHA + 10% DCC, and 3% MeHA + 10% DVC groups exhibited a measurable yield stress, whereas all groups had a measurable storage modulus. Data are reported as mean + standard deviation ($n = 5$); *significantly different from 3% MeHA acellular group ($p < 0.05$); #significantly different from 3% MeHA + 10% DCC acellular group ($p < 0.05$); \$significantly different from 10% DCC group ($p < 0.05$); &significantly different from all other groups ($p < 0.05$).



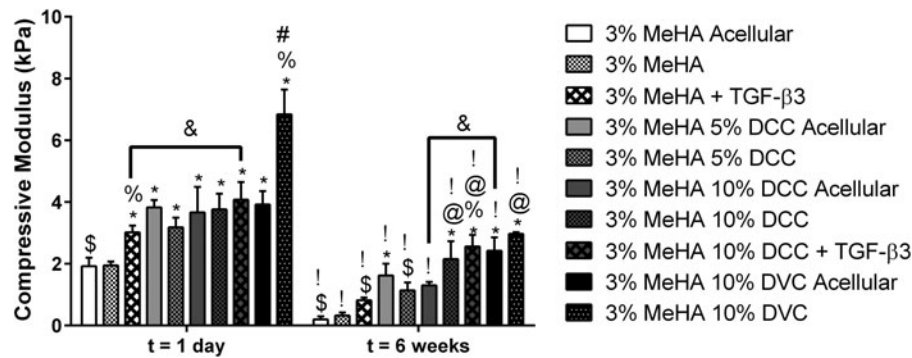


FIG. 4. Compressive moduli of crosslinked hydrogels after 1 day and 6 weeks of culture. Gels containing at least 10% DCC or DVC microparticles had significantly larger moduli than 3% MeHA gels alone. Data are reported as mean + standard deviation ($n=5$); *significantly different from 3% MeHA at same time point ($p<0.05$); %significantly different from acellular group of same formulation at same time point ($p<0.05$); #significantly different from all other groups at same time point ($p<0.05$); \$significantly different from 3% MeHA + 10% DCC at same time point ($p<0.05$); @significantly different from 3% MeHA + TGF- β_3 and 3% MeHA + 5% DCC at same time point ($p<0.05$); & $p<0.05$ for specified comparison; 'significantly different from same group at first time point ($p<0.05$). TGF- β_3 , transforming growth factor- β_3 .

Mechanical testing of crosslinked hydrogels

One day after crosslinking, all of the groups except for the acellular MeHA group had a compressive modulus significantly higher than that of the MeHA group ($p<0.05$), which had a compressive modulus of 1.94 ± 0.13 kPa (Fig. 4). The compressive modulus of the MeHA + DVC group was 6.82 ± 0.79 kPa (Fig. 4), which was 3.5, 2.2, and 1.8 times larger than the compressive moduli of MeHA, MeHA + 5% DCC, and MeHA + 10% DCC groups, respectively ($p<0.05$). Furthermore, the modulus of the MeHA + DVC group was 2.3 and 1.7 times larger than that of the MeHA + TGF- β_3 and MeHA + 10% DCC + TGF- β_3 groups, respectively. Finally, the moduli of the MeHA + DVC and MeHA + TGF- β_3 groups were 1.7 and 1.6 times, respectively, larger than those of their acellular controls ($p<0.05$).

At 6 weeks, the MeHA + 5% DCC acellular group, both cellular groups composed of MeHA + 10% DCC, and the DVC groups had at least four times larger compressive moduli than that of the MeHA group, which had a compressive modulus of 0.31 ± 0.13 kPa ($p<0.05$). The MeHA + DVC group had a compressive modulus of 2.964 ± 0.056 kPa, which was 9.1 times larger than that of the MeHA group ($p<0.05$), but was not significantly different from that of the MeHA + 10% DCC + TGF- β_3 group. The modulus of the MeHA + 10% DCC + TGF- β_3 group was 2.55 ± 0.39 kPa, which was two times larger than that of its acellular control ($p<0.05$). The MeHA + DVC acellular group had a compressive modulus of 2.40 ± 0.44 kPa, which was 1.9 times larger than that of the MeHA + 10% DCC group ($p<0.05$) (Fig. 4).

Over the 6 week culture period, all of the groups had a significant reduction in their compressive moduli ($p<0.05$). However, although the acellular MeHA, MeHA, and MeHA + TGF- β_3 groups experienced 90%, 83%, and 73% respective reductions in their compressive moduli over the culture period ($p<0.05$), all of the other groups experienced less than 65% reductions in their respective compressive moduli ($p<0.05$). At 6 weeks, the compressive modulus of the MeHA + 10% DCC + TGF- β_3 group was 37% less than its original value at day 1 ($p<0.05$), whereas the modulus of its respective acellular group was 64% less than its original value ($p<0.05$) (Fig. 4).

Swelling and volume analysis of crosslinked hydrogel pastes

After swelling to equilibrium for 24 h, the swelling degree of the MeHA group was 34 ± 13 (Fig. 5A). The only groups that had significantly smaller swelling degrees were the MeHA + 10% DCC acellular group and the MeHA + DVC acellular and cellular groups, which had swelling degrees of 17.9 ± 3.1 , 15.6 ± 1.3 , and 13.27 ± 0.88 , respectively ($p<0.05$) (Fig. 5A).

At day 1 after crosslinking, none of the gel volumes deviated significantly from the volume of the MeHA group, which was 40.5 ± 2.7 μ L ($p<0.05$) (Fig. 5B). However, at 6 weeks after crosslinking, the MeHA group had a volume of 82.7 ± 11.6 μ L. The volumes of the MeHA + 5% DCC, MeHA + 10% DCC, and MeHA + DVC were 26%, 31.5%, and 43% lower than that of the MeHA group, respectively ($p<0.05$) (Fig. 5B). In addition, the volume of the MeHA + TGF- β_3 group was 20.5% and 21.2% lower than that of the MeHA acellular and cellular groups, respectively ($p<0.05$). The DVC group was not significantly different from the MeHA + 10% DCC + TGF- β_3 group, but the volume of the MeHA + 10% DCC + TGF- β_3 group was 31% less and 20% less than that of the MeHA + TGF- β_3 and the MeHA + 10% DCC groups, respectively.

Over the 6 week culture period, the volumes of all gels, with the exception of the MeHA + 10% DCC + TGF- β_3 and the acellular MeHA + DVC groups, increased significantly ($p<0.05$). The volume of the MeHA group increased by 2.1 times compared with its original volume, whereas the volumes of the MeHA + TGF- β_3 , the MeHA + 5% DCC, and the MeHA + 10% DCC groups only increased by 49%, 47%, and 45%, respectively ($p<0.05$) (Fig. 5B).

Biochemical content of crosslinked hydrogels

All of the cellular groups had significantly higher DNA content than their respective acellular groups at all time points ($p<0.05$). At day 1 after crosslinking, the MeHA + 10% DCC group had 570 ± 130 ng DNA per gel, and the only gels with a significantly different DNA content from this group were the MeHA + 10% DCC + TGF- β_3 and MeHA + DVC groups, which had DNA contents 45% and

FIG. 5. Swelling degree (A) and volume (B) of crosslinked hydrogels. The only gels with significantly smaller swelling degrees than the 3% MeHA gels were the 3% MeHA + 10% DCC acellular group and the 3% MeHA + 10% DVC acellular and cellular groups. At day 1, there were no significant differences between groups. However, the inclusion of DCC or DVC or exposure to TGF- β_3 significantly reduced the volume at 6 weeks. Data are reported as mean + standard deviation ($n=5$); *significantly different from 3% MeHA at same time point ($p<0.05$); %significantly different from acellular group of same formulation at same time point ($p<0.05$); \$significantly different from 3% MeHA + 10% DCC at same time point ($p<0.05$); !significantly different from same group at first time point ($p<0.05$).

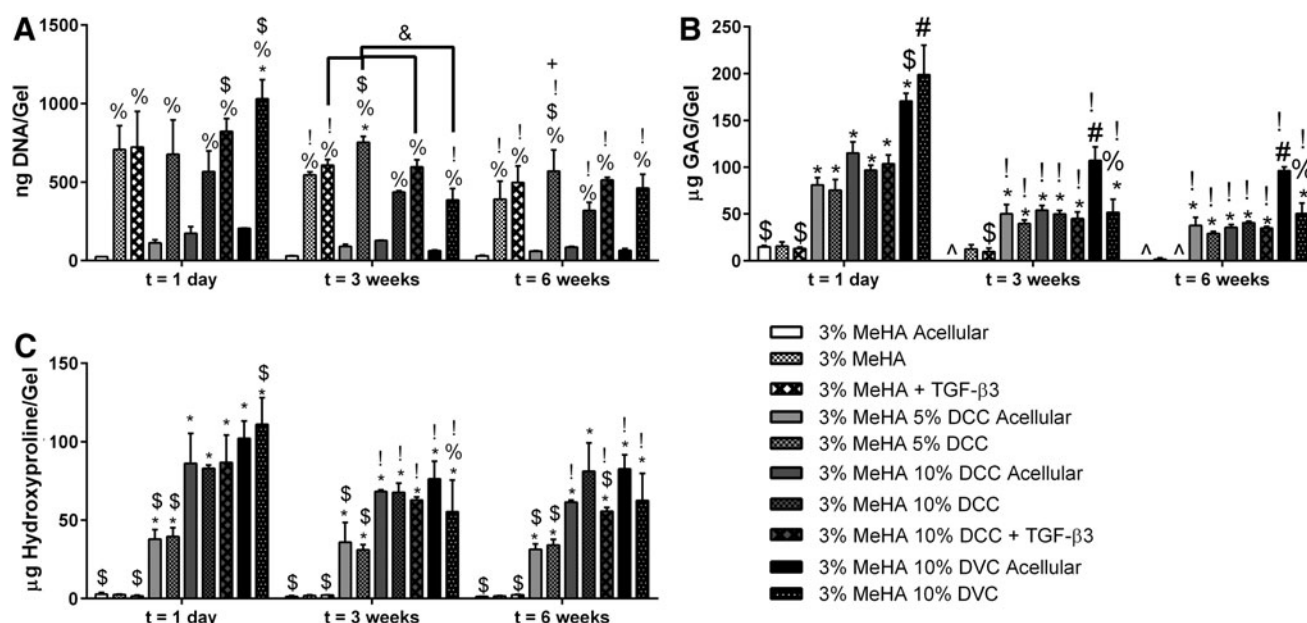
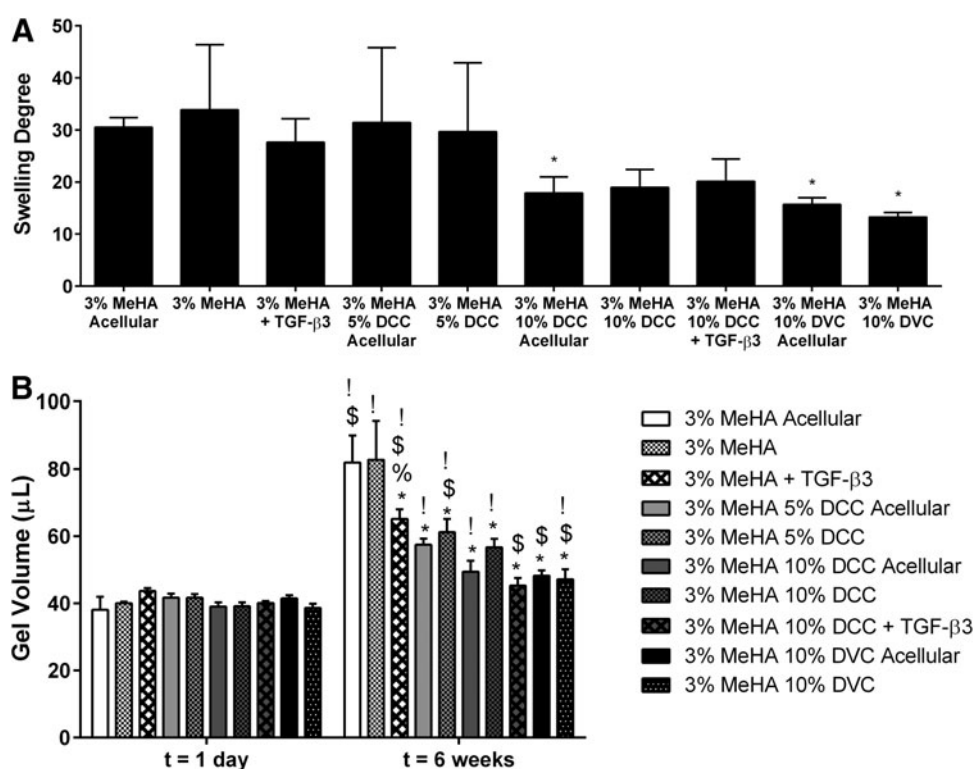


FIG. 6. Biochemical content of gels over the 6 week culture period. (A) DNA content, (B) GAG content, and (C) hydroxyproline content. All gels contained significantly higher DNA content than their respective acellular groups at all time points, and all gels containing DCC or DVC had significant reductions in GAG over the 6 week culture period. Data are reported as mean + standard deviation ($n=5$); ^below detectable limit; *significantly different from 3% MeHA at same time point ($p<0.05$); %significantly different from acellular group of same formulation at same time point ($p<0.05$); #significantly different from all other groups at same time point ($p<0.05$); \$significantly different from 3% MeHA + 10% DCC at same time point ($p<0.05$); !significantly different from same group at first time point ($p<0.05$); +significantly different from same group at previous time point ($p<0.05$).

82% higher per gel, respectively ($p < 0.05$) (Fig. 6A). There was no significant difference between the MeHA+10% DCC+TGF- β_3 and MeHA+DVC groups, however. At 3 weeks after crosslinking, the MeHA+DVC group had a DNA content of 386 ± 73 ng DNA per gel, which was 36%, 49%, and 35% less than the DNA content of the MeHA+TGF- β_3 , MeHA+5% DCC, and MeHA+10% DCC+TGF- β_3 groups, respectively ($p < 0.05$) (Fig. 6A). There was no significant difference between the MeHA+DVC group and the MeHA+10% DCC group, however. After 6 weeks of culture, the MeHA+5% DCC group contained 1.8 times more DNA than the MeHA+10% DCC group ($p < 0.05$) (Fig. 6A). However, no other cellular groups were significantly different from the MeHA+10% DCC group.

Over the course of the 6 week culture period, all of the cellular groups had a significant reduction in DNA content ($p < 0.05$), where the DNA content in the MeHA, MeHA+TGF- β_3 , MeHA+5% DCC, MeHA+10% DCC, MeHA+10% DCC+TGF- β_3 , and MeHA+DVC groups reduced by 45%, 31%, 16%, 43%, 38%, and 55% compared with their original DNA contents, respectively ($p < 0.05$). The acellular groups did not have any significant reduction in DNA content over the culture period (Fig. 6A).

All of the groups with DCC and DVC had significantly higher initial GAG contents at day 1 than the MeHA group ($p < 0.05$), which had a GAG content of 15.5 ± 4.6 μ g GAG per gel. Compared with the GAG content of the MeHA group, the GAG content of the MeHA+5% DCC, MeHA+10% DCC, MeHA+10% DCC+TGF- β_3 , and MeHA+DVC groups were 4.9, 6.3, 6.7, and 12.9 times larger, respectively (Fig. 6B).

At day 1, the GAG content of the MeHA+DVC group was 16.6% higher than that of its respective acellular group ($p < 0.05$). Furthermore, the GAG content of the MeHA+DVC group was 15, 2.1, and 1.9 times larger than that of the MeHA+TGF- β_3 , MeHA+10% DCC, and the MeHA+10% DCC+TGF- β_3 groups, respectively.

At 3 weeks, all of the groups with DCC and DVC contained significantly larger GAG contents than the MeHA group ($p < 0.05$), which had a GAG content of 12.5 ± 4.6 μ g GAG per gel. The GAG contents of the MeHA+5% DCC, MeHA+10% DCC, MeHA+10% DCC+TGF- β_3 , and MeHA+DVC groups were 3.2, 4, 3.6, and 4.1 times larger than that of MeHA group, respectively (Fig. 6B). In addition, the GAG content of the MeHA+DVC group was 52% less than that of its respective acellular control ($p < 0.05$). Furthermore, there were no significant differences among the MeHA+DVC, the MeHA+10% DCC+TGF- β_3 , and the MeHA+10% DCC groups.

At 6 weeks, again all of the groups with DCC and DVC contained significantly larger GAG content than the MeHA group ($p < 0.05$), which had a GAG content of 1.7 ± 1.2 μ g GAG per gel. Compared with the GAG content of the MeHA group, the GAG content of the MeHA+5% DCC, MeHA+10% DCC, MeHA+10% DCC+TGF- β_3 , and MeHA+DVC groups was 17, 24, 20, and 29 times larger, respectively (Fig. 6B). The GAG content of the MeHA+DVC group was 48% less than that of its respective acellular control ($p < 0.05$), but there were no significant differences among the MeHA+DVC, the MeHA+10% DCC+TGF- β_3 , and the MeHA+10% DCC groups.

Over the 6 week culture period, all of the groups with DCC and DVC had significant reductions in GAG content,

where the GAG content of the MeHA+5% DCC acellular and cellular groups, the MeHA+10% DCC acellular, cellular, and TGF- β_3 -exposed groups, and the acellular and cellular MeHA+DVC groups reduced by 54%, 62%, 69%, 58%, 66%, 44%, and 75%, respectively.

Furthermore, all of the groups with DCC and DVC had significantly higher initial hydroxyproline content at day 1 than the MeHA group ($p < 0.05$), which had a content of 2.57 ± 0.23 μ g hydroxyproline per gel. Compared with the hydroxyproline content of the MeHA group, the hydroxyproline content of the MeHA+5% DCC, MeHA+10% DCC, MeHA+10% DCC+TGF- β_3 , and MeHA+DVC groups was 15, 32, 34, and 43 times larger, respectively (Fig. 6C).

At day 1, the hydroxyproline content of the MeHA+DVC group was 1.3 times higher than that of the MeHA+10% DCC group ($p < 0.05$). In addition, the MeHA+10% DCC group contained 2.1 times the amount of hydroxyproline of the MeHA+5% DCC group ($p < 0.05$).

At 3 weeks, all of the DCC and DVC groups contained significantly larger hydroxyproline contents than the MeHA group ($p < 0.05$), which contained 1.90 ± 0.40 μ g hydroxyproline per gel. Compared with the hydroxyproline content of the MeHA group, the hydroxyproline content of the MeHA+5% DCC, MeHA+10% DCC, MeHA+10% DCC+TGF- β_3 , and MeHA+DVC groups was 16, 36, 33, and 29 times larger, respectively (Fig. 6C). In addition, the hydroxyproline content of the MeHA+DVC group was 27.4% less than that of its respective acellular control ($p < 0.05$), and the MeHA+10% DCC group contained 2.2 times the amount of hydroxyproline found in the MeHA+5% DCC group ($p < 0.05$). However, there were no significant differences among the MeHA+DVC, the MeHA+10% DCC, and the MeHA+10% DCC+TGF- β_3 groups.

At 6 weeks, again all of the groups with DCC and DVC contained significantly larger hydroxyproline content than the MeHA group ($p < 0.05$), which contained 1.64 ± 0.24 μ g hydroxyproline per gel. Compared with the hydroxyproline content of the MeHA group, the hydroxyproline content of the MeHA+5% DCC, MeHA+10% DCC, MeHA+10% DCC+TGF- β_3 , and MeHA+DVC groups was 21, 49, 34, and 38 times larger, respectively (Fig. 6C). The hydroxyproline content of the MeHA+10% DCC group was 2.4 and 1.5 times larger than that of the MeHA+5% DCC and MeHA+10% DCC+TGF- β_3 groups, respectively ($p < 0.05$). However, there was no significant difference between the MeHA+DVC and the MeHA+10% DCC+TGF- β_3 groups.

Over the 6 week culture period, the groups that did not have a significant reduction in hydroxyproline content were all three MeHA groups, both MeHA+5% DCC groups, and the MeHA+10% DCC group. The hydroxyproline content of the MeHA+DVC group reduced to 56% of its original content over the 6 weeks period ($p < 0.05$).

Gene expression

Throughout the entire culture period, the MeHA+5% DCC and MeHA+10% DCC groups never expressed collagen II. At day 1, the rest of the groups did not have any significant differences. At 1 week, the MeHA+TGF- β_3 group did not express collagen II, and there were no significant differences in expression between the remaining groups. At 2 weeks, the only groups expressing collagen II were the MeHA+10% DCC+

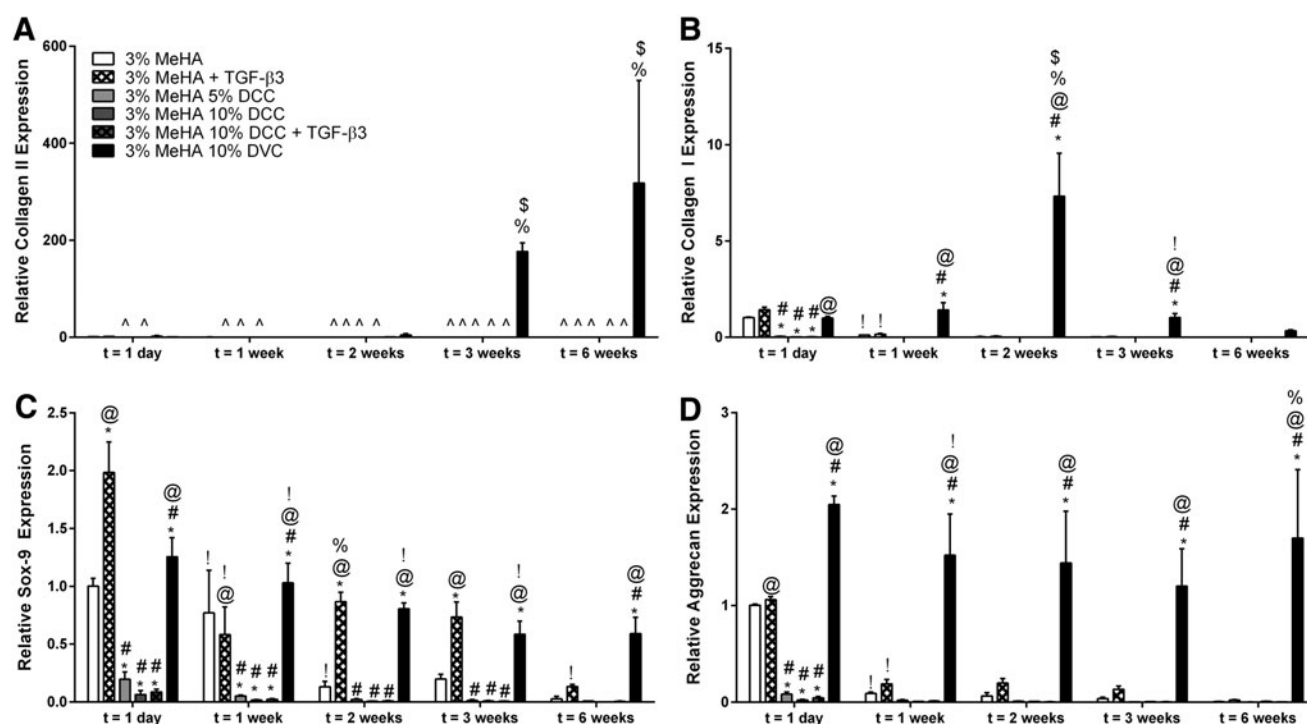


FIG. 7. Relative gene expression of (A) collagen II, (B) collagen I, (C) Sox-9, and (D) aggrecan. The DVC group consistently outperformed the other groups in collagen II, Sox-9, and aggrecan expression, even when compared with TGF- β_3 exposed groups. Data are reported as mean + standard deviation ($n=5$); *significantly different from 3% MeHA at same time point ($p<0.05$); #significantly different from 3% MeHA + TGF- β_3 at same time point ($p<0.05$); @significantly different from all DCC-containing groups at same time point ($p<0.05$); %significantly higher than same group at previous time point ($p<0.05$); \$significantly higher than same group at first time point ($p<0.05$); !significantly lower than same group at previous time point ($p<0.05$); ^expression not detected.

TGF- β_3 and the MeHA + DVC groups, although the difference between them was not significant. At 3 and 6 weeks, the only group expressing collagen II was the MeHA + DVC group, which had a relative collagen II expression that was 180 and 320 times larger than that of the calibrator group (i.e., MeHA group at day 1), respectively ($p<0.05$) (Fig. 7A).

At day 1, the DCC-containing groups had at least 98% less collagen I expression than the MeHA group ($p<0.05$) (Fig. 7B). By 2 weeks, the relative collagen I expression of MeHA + DVC increased to 304 times the MeHA group value. However, that expression significantly decreased by 86% at 3 weeks, but was still 99 times larger than the relative expression of the MeHA group. Although the collagen I expression reduced significantly from day 1 to 1 week for both the cellular and acellular MeHA groups ($p<0.05$), the collagen I expression for these and all groups but the MeHA + DVC groups remained steady during the rest of the 6 weeks.

The MeHA + TGF- β_3 and MeHA + DVC groups had significantly higher Sox-9 expression than the groups containing DCC from day 1 to 3 weeks, where the relative expression was 2 and 1.3 times the MeHA group, respectively, at day 1, and was 3.7 and 3 times larger than the MeHA group at 3 weeks ($p<0.05$) (Fig. 7C). At 6 weeks, the DVC group had significantly higher Sox-9 expression than all other groups, where its expression was 4.4 and 109 times higher than that of the MeHA + TGF- β_3 and the MeHA + 10% DCC + TGF- β_3 groups, respectively ($p<0.05$).

At day 1, the relative aggrecan expression of the DCC-containing groups was significantly lower than that of the MeHA group, whereas the relative expression of the MeHA + DVC group was two times higher than that of the MeHA group ($p<0.05$) (Fig. 7D). Over the culture period, both the cellular and acellular MeHA groups significantly reduced their aggrecan expression; however, the aggrecan expression of the MeHA + DVC group remained significantly higher than that of MeHA and all DCC groups over the 6 weeks ($p<0.05$). In addition, the MeHA + DVC group's relative aggrecan expression was 2, 17, 22, 34, and 410 times higher than that of MeHA at day 1, 1 week, 2 weeks, 3 weeks, and 6 weeks, respectively ($p<0.05$). Lastly, the relative aggrecan expression of the MeHA + DVC group at 6 weeks was 80 and 585 times higher than that of the MeHA + TGF- β_3 and the MeHA + 10% DCC + TGF- β_3 groups, respectively.

Histological evaluation

Saf-O staining did not reveal an increase in Saf-O staining intensity over the culture period. However, at 6 weeks, some nodular Saf-O staining was noted in the MeHA + TGF- β_3 group (Fig. 8). All DCC- and DVC-containing groups stained for collagen II; however, no changes were noted in the location and intensity of collagen II staining over the culture period (Fig. 8).

Collagen I staining was noted again in all of the DCC- and DVC-containing groups. However, the intensity of

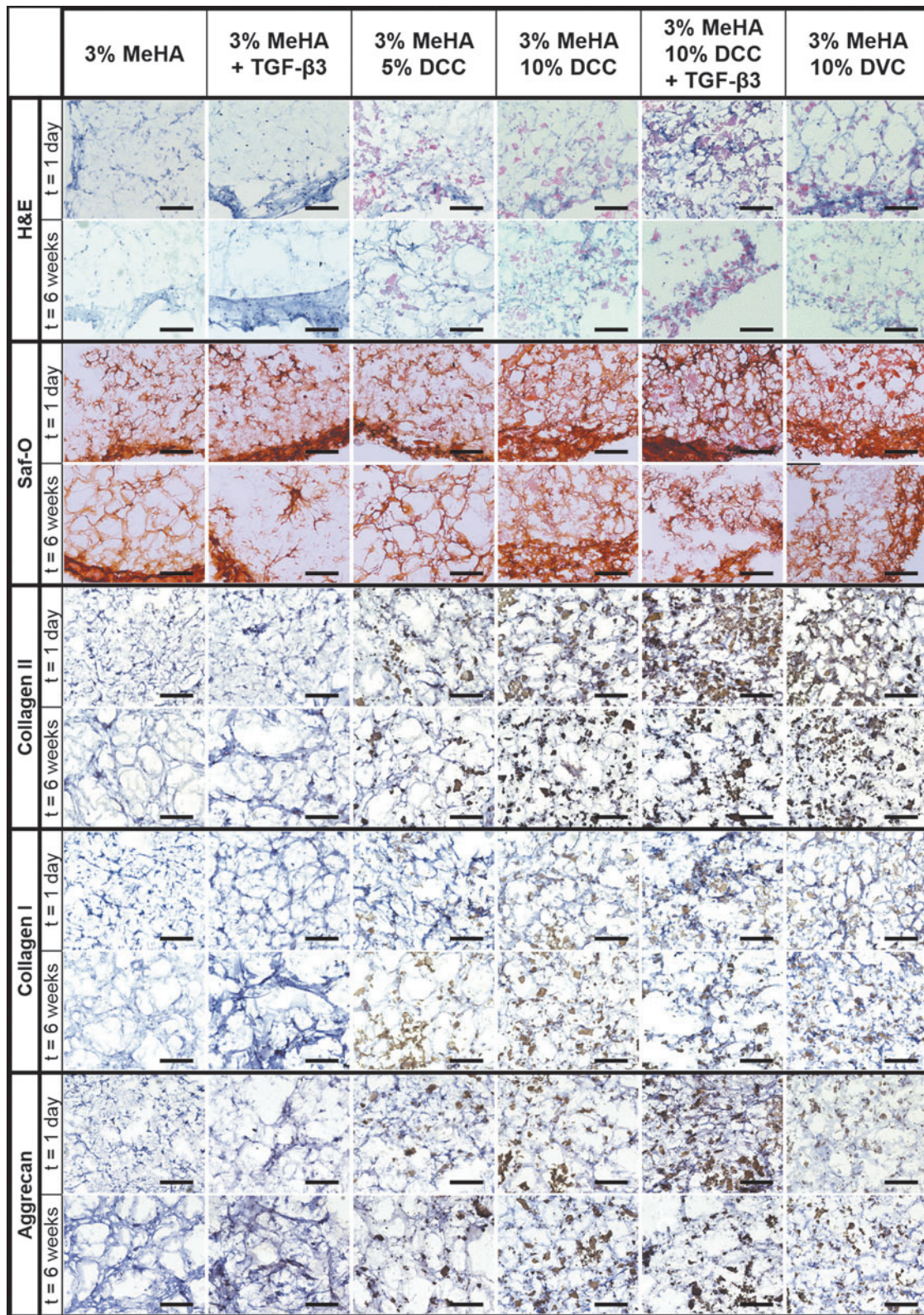


FIG. 8. Histological analysis of gels. All gels stained *red/orange* for GAGs, although no increase in the amount of staining was noted over the culture period. However, nodular Saf-O staining was noted in the 3% MeHA + TGF- β_3 group. All DCC- and DVC-containing groups were stained for collagen II; however, no changes were noted in the location and intensity of collagen II staining over the culture period. Collagen I staining was noted again in all DCC- and DVC-containing groups. However, the intensity of collagen I staining decreased over the culture period for the 3% MeHA + 5% DCC and 3% MeHA + 10% DCC groups and appeared to increase slightly for the 3% MeHA + 10% DVC group. Aggrecan staining was noted in all DCC- and DVC-containing groups, where the aggrecan staining became more intense near the DCC and DVC microparticles in the 3% MeHA + 10% DCC + TGF- β_3 and 3% MeHA + 10% DVC groups over the culture period. Scale bars are 200 μ m. Color images available online at www.liebertpub.com/tea

collagen I staining decreased over the culture period for the MeHA + 5% DCC and MeHA + 10% DCC groups (Fig. 8). The intensity of the collagen I staining appeared to increase slightly for the MeHA + DVC group. This slight increase in intensity was noted near and within the DVC microparticles. Aggrecan staining was noted in all DCC- and DVC-containing groups, where notably the aggrecan staining became more intense near the DCC and DVC microparticles in the MeHA + 10% DCC + TGF- β_3 and MeHA + DVC groups over the culture period (Fig. 8).

Discussion

We have introduced not only a method to overcome the drawbacks of implanting hydrogels *in situ* (i.e., leaking from the defect site), but in addition, we have introduced a method to induce chondrogenesis of cells encapsulated within the networks. Previous studies have explored the chondrogenic potential of DCC and DVC.^{8,26–30} Cheng *et al.*³⁰ reported using a porous cartilage matrix composed of homogenized and then lyophilized DVC matrix, of which chondrogenesis was observed even without growth factor supplementation. However, these matrices succumbed to cell-mediated contraction, but when the matrices were further crosslinked with genipin, they found that the materials did not exhibit contraction and were chondroinductive.⁸ The same group infiltrated cartilage matrix with woven poly(ϵ -caprolactone) and observed cartilaginous matrix production.²⁸ Zheng *et al.*²⁶ reported using DCC to create nanofibrous ECM scaffolds that induced mesenchymal stem cell chondrogenesis. Our group was the first to explore the short-term chondrogenic potential of DCC versus DVC.¹⁷ However, for the first time in this study, not only were DVC and DCC compared for their long-term chondrogenic potential, but they were also evaluated for their ability to exhibit a yield stress in hydrogel precursor solutions. In this study, chondrogenesis was induced through incorporating native cartilage ECM into the MeHA/cartilage matrix gel networks, which furthermore resulted in the paste-like behavior and yield stress that was observed before crosslinking. The yield stress denotes the threshold where a solution transitions between an elastic solid and a pseudoplastic liquid, and exhibiting a yield stress is crucial because it will prevent the hydrogel precursor from flowing away, keeping the material at the site of interest until crosslinking. In a surgical context, a material that exhibits a yield stress would allow a surgeon to appropriately shape and contour the material to the defect site before crosslinking it in place. The paste-like precursor solutions were able to obtain yield stresses of more than 200 Pa with MeHA mixed with DVC microparticles. For context, the yield stress for a common paste-like material such as toothpaste is approximately 200 Pa. However, we did not achieve toothpaste consistency with the incorporation of DCC microparticles, although we still noted that these materials did have a yield stress. Although at this point without further testing it is uncertain why the DCC microparticles did not impart as high of a yield stress on the pastes as the DVC microparticles, the SEM images revealed subtle differences between the DCC and DVC, which may provide clues to understanding the observed rheological differences. A grain-like appearance was noted only on the DCC and that the DCC microparticles had, in general, smoother surfaces than the DVC microparticles. Because it is

known that decellularization can result in changes in matrix architecture and surface ligand landscape,²¹ it is possible that these entities were altered in the decellularization process, and thus the decellularization process may have played a role in the reduction of yield stress that we observed. It was noted that the yield stress of DCC microparticles alone was higher than the yield stress of MeHA combined with the DCC, and this reduction in yield stress when MeHA and particles were combined differs from what was noted in previous work, where a 3.4-fold increase was observed in the yield stress of hyaluronic acid nanoparticles combined with MeHA in comparison with the nanoparticles alone, where the MeHA alone had no measurable yield stress.³ That work suggested that the hyaluronic acid nanoparticles had some physical or chemical interactions with the MeHA in addition to the interactions with the other nanoparticles, whereas in this study, the interactions between particles and MeHA were likely negligible. Of concern is that when rBMSCs were mixed in with the DCC group, the precursor had no measurable yield stress, although it still exhibited some viscoelastic behavior, evident by its measurable storage modulus and macroscopically observed non-Newtonian behavior. Lastly, although it was not performed in this study, future quantification of syringeability would be of value.

In addition to DVC having superior rheological properties, the DVC invoked superior chondroinductivity than DCC microparticles. For collagen II, Sox-9, and aggrecan expression, the MeHA + DVC group repeatedly outperformed the DCC-containing groups, even when the DCC groups were exposed to TGF- β_3 . Interestingly, we only performed a mild decellularization by removing only 44% of the initial DNA, 23% of the initial GAG, and 23% of the initial hydroxyproline, and even though the initial biochemical contents were not drastically altered, the cellular response to these materials was severely affected. The current finding of DVC outperforming DCC in chondroinduction is in contradiction to our previously reported increase in chondroinductivity of DCC over DVC,¹⁷ but we hypothesize that the differences between the previous and this study are that, currently, rBMSCs were encapsulated within a 3D scaffold rather than studied in pellet culture and the long-term gene expression over a 6 week period rather than only 1 week as in the prior study was observed. Moreover, under biochemical and histological analysis, other than a slight increase in aggrecan staining near the cartilage microparticles over the 6 week culture period, significant tissue synthesis overall was not observed, which suggests that although the cells may have been chondroinduced, they were not actively secreting large amounts of cartilage matrix. However, it is possible that either some of the matrix was being remodeled so a net increase in the amount of staining could not be observed even though matrix secretion might have been present, or a net increase was not able to be detected because of the large amount of matrix initially present in the hydrogel. Ultimately, without further testing, it still remains unclear as to whether decellularization is necessary for cartilage tissue engineering.

The question of whether or not decellularization is needed is complex and will depend upon each application of cartilage ECM. It has been established that cells exposed to a target ECM will more easily differentiate toward the target tissue,^{31,32} where one of the reasons for this ECM-specific

differentiation may be because native ECM may have the potential to retain the growth factors that will steer the differentiation toward the specific target tissue.⁴ Decellularizing cartilage ECM may not only alter the matrix architecture but it may also furthermore remove some of these important growth factors, affecting the bioactivity of the cartilage ECM. Furthermore, altering the architecture may hinder growth factor retention. For example, proteoglycans, specifically aggrecan in cartilage matrix, are well known for how they affect the mechanical properties of tissues and found extensively in native cartilage matrix and are thought to be a reservoir of several growth factors,^{33,34} and thus, the preservation of these proteoglycans may be crucial to successful tissue regeneration. Therefore, although we are still in the beginning stages of determining the appropriate ECM processing protocol for cartilage tissue, it may prove to be ideal to use unaltered, non-DCC tissue for certain applications. Applications such as cell-derived matrix, where cartilage ECM can be grown from a patient's own cells,¹² would not need to be decellularized since the tissue source would be autogenous. In addition, through the successful use of allograft cartilage as evidenced by the success of current allograft products like Zimmer's DeNovo, if the cartilage tissue would be used for articular cartilage applications, it may not need to be decellularized.

However, on the opposing side of whether or not to decellularize cartilage tissue are cases where cartilage is being used for bone regeneration through endochondral ossification. In these applications where the cartilage will be more exposed to host immunogenic cells,³⁵ decellularization may be necessary. In addition, decellularization may be necessary for cartilage derived from xenogeneic sources. In this study, we used porcine cartilage as proof of concept for comparing DCC with DVC. However, ultimately it may or may not be desired to use xenograft sources for future work. Using xenografts comes with its own challenges, such as the need to remove the alpha-Gal epitope, a carbohydrate found within xenograft ECM that is known to cause graft failure if not successfully removed.¹²

Although graft failure can be caused through biochemical entities, it is possible for graft failure to occur biomechanically. For this reason, we tested the mechanical and swelling properties of DCC- and DVC-incorporated hydrogel networks after crosslinking. Native cartilage is ~80% water, which equates to a swelling degree of ~5, and has an elastic compressive modulus ranging from 240 to 1000 kPa.^{36–38} However, it must be noted that the biomechanical properties can vary depending on parameters such as the method of testing, the strain rate of testing, and cartilage zone depth.³⁹ In this work, the swelling degree was significantly lowered from more than 30 to between 10 and 20 by incorporating 10% DCC or DVC. For tissue engineering, it is neither desired for scaffold constructs to swell from the defect site nor is it desirable for the constructs to shrink within the defect site, because in both instances it can cause disintegration of the scaffold with host tissue, and thus may hinder cartilage regeneration.⁸ In this study, it was noted that the inclusion of DVC resulted in the gels retaining their original volumes throughout culture. However, it was noted that the elastic compressive moduli obtained in this study (ranging from ~2 to 8 kPa at day 1) were nowhere near that of native cartilage. Including DCC and DVC

with MeHA significantly increased the compressive modulus. Interestingly, encapsulation of DVC and cells together significantly increased the compressive modulus compared with that of the acellular MeHA+DVC control and all MeHA+DCC groups, which suggests that there may be superior cell-matrix interaction by incorporating DVC rather than DCC with cells and gives further reasoning to support the use of DVC over DCC. Overall, in this study, although incorporating DVC and DCC may prove to be beneficial for tissue engineering, to ultimately obtain mechanical properties to that of native cartilage ECM, it may be necessary to increase the degree of methacrylation or to change the photocrosslinkable polymer to a polymer that has an inherently higher compressive modulus.⁴⁰

Conclusions

ECM-based materials are gaining widespread attention in the regenerative medicine field and they continue to show great promise toward cartilage regeneration applications. In this study, cartilage matrix microparticles not only induced cells to differentiate toward a chondrogenic lineage but they also concurrently provided the hydrogel precursor solutions with a yield stress (i.e., paste-like consistency), which translates to a tremendous advantage for material placement in clinical applications. In addition, although significant emphasis has been placed on the necessity to decellularize ECM components that are used in regenerative medicine products, we challenged that paradigm by providing the first direct comparison of the long-term bioactivity of DCC and DVC and thereby demonstrating that DVC may be superior in promoting chondrogenesis than DCC. Moreover, DVC consistently outperformed all TGF- β_3 -exposed groups in aggrecan and collagen II gene expression, which may present significant advantages in cost and regulatory approval of chondroinductive strategies for cartilage regeneration because of eliminating the need for costly growth factors.⁴¹ Certainly, future work will need to address improving the mechanical properties of these networks, whereby choosing a higher mechanically performing hydrogel, such as an interpenetrating network hydrogel,^{42–46} could be considered. In addition, overall matrix production will need to be addressed, where *in vivo* studies will be paramount because immunogenicity as well as how biomechanical stimulation of DCC and DVC may affect chondroinductivity and therefore, hyaline-like cartilage regeneration can be tested. Furthermore, the reproducibility and shelf life of these materials must be tested because the heterogeneity of cartilage matrix and differences in the quality of cartilage ECM from one hog to another may vary and may affect the ability to reproduce similar particles every time. Overall, the results of this study suggest that DVC may be a promising chondroinductive material for some cartilage tissue engineering strategies.

Acknowledgments

We acknowledge funding support from the NIH (R01 DE022472 to C.J.B., S10 RR024664) and the NSF for a Graduate Research Fellowship (E.B.) and an NSF Major Research Instrumentation Grant (0320648), and the Kansas Bioscience Authority Rising Star Award (M.D.). In addition, we gratefully thank Heather Shinogle from the

Microscopy Laboratory for assistance with imaging, Francisca Acosta and Emi Kiyotake for their assistance with IHC, and the members of the KU Biomaterials and Tissue Engineering laboratory who helped with the porcine cartilage harvesting.

Disclosure Statement

No competing financial interests exist.

References

1. Rughani, R.V., Branco, M.C., Pochan, D.J., and Schneider, J.P. De novo design of a shear-thin recoverable peptide-based hydrogel capable of intrafibrillar photopolymerization. *Macromolecules* **43**, 7924, 2010.
2. Todd, R.H., and Daniel, S.K. Hydrogels in drug delivery: progress and challenges. *Polymer* **49**, 1993, 2008.
3. Beck, E.C., Lohman, B.L., Tabakh, D.B., Kieweg, S.L., Gehrke, S.H., Berkland, C.J., and Detamore, M.S. Enabling surgical placement of hydrogels through achieving paste-like rheological behavior in hydrogel precursor solutions. *Ann Biomed Eng* **43**, 2569, 2015.
4. Benders, K., van Weeren, P., Badylak, S., Saris, D., Dhert, W., and Malda, J. Extracellular matrix scaffolds for cartilage and bone regeneration. *Trends Biotechnol* **31**, 169, 2013.
5. Burdick, J.A., Mauck, R.L., Gorman, J.H., III, and Gorman, R.C. Cellular biomaterials: an evolving alternative to cell-based therapies. *Sci Transl Med* **5**, 176ps4, 2013.
6. Renth, A.N., and Detamore, M.S. Leveraging "raw materials" as building blocks and bioactive signals in regenerative medicine. *Tissue Eng Part B Rev* **18**, 341, 2012.
7. Cha, M., Do, S., Park, G., Du, P., Han, K.-C., Han, D., and Park, K. Induction of re-differentiation of passaged rat chondrocytes using a naturally obtained extracellular matrix microenvironment. *Tissue Eng Part A* **19**, 978, 2013.
8. Cheng, N.-C., Estes, B., Young, T.-H., and Guilak, F. Genipin-crosslinked cartilage-derived matrix as a scaffold for human adipose-derived stem cell chondrogenesis. *Tissue Eng Part A* **19**, 484, 2013.
9. Decaris, M., Binder, B., Soicher, M., Bhat, A., and Leach, J. Cell-derived matrix coatings for polymeric scaffolds. *Tissue Eng Part A* **18**, 2148, 2012.
10. Schwarz, S., Koerber, L., Elsaesser, A.F., Goldberg-Bockhorn, E., Seitz, A.M., Durselen, L., Ignatius, A., Walther, P., Breiter, R., and Rotter, N. Decellularized cartilage matrix as a novel biomatrix for cartilage tissue-engineering applications. *Tissue Eng Part A* **18**, 2195, 2012.
11. Yang, Z., Shi, Y., Wei, X., He, J., Yang, S., Dickson, G., Tang, J., Xiang, J., Song, C., and Li, G. Fabrication and repair of cartilage defects with a novel acellular cartilage matrix scaffold. *Tissue Eng Part C Methods* **16**, 865, 2010.
12. Sutherland, A.J., Converse, G.L., Hopkins, R.A., and Detamore, M.S. The bioactivity of cartilage extracellular matrix in articular cartilage regeneration. *Adv Healthc Mater* **4**, 29, 2015.
13. Cheng, N.-C., Estes, B.T., Young, T.-H., and Guilak, F. Engineered cartilage using primary chondrocytes cultured in a porous cartilage-derived matrix. *Regen Med* **6**, 81, 2011.
14. Garrigues, N.W., Little, D., Sanchez-Adams, J., Ruch, D.S., and Guilak, F. Electrospun cartilage-derived matrix scaffolds for cartilage tissue engineering. *J Biomed Mater Res A* **102**, 3998, 2014.
15. Levorson, E., Hu, O., Mountziaris, P., Kasper, F., and Mikos, A. Cell-derived polymer/extracellular matrix composite scaffolds for cartilage regeneration, part 2: construct devitalization and determination of chondroinductive capacity. *Tissue Eng Part C Methods* **20**, 358, 2014.
16. Schwarz, S., Elsaesser, A.F., Koerber, L., Goldberg-Bockhorn, E., Seitz, A.M., Bermueller, C., Durselen, L., Ignatius, A., Breiter, R., and Rotter, N. Processed xenogenic cartilage as innovative biomatrix for cartilage tissue engineering: effects on chondrocyte differentiation and function. *J Tissue Eng Regen Med* **9**, E239, 2015.
17. Sutherland, A.J., Beck, E.C., Dennis, S.C., Converse, G.L., Hopkins, R.A., Berkland, C.J., and Detamore, M.S. Decellularized cartilage may be a chondroinductive material for osteochondral tissue engineering. *PLoS One* **10**, 2015.
18. Keane, T.J., Londono, R., Turner, N.J., and Badylak, S.F. Consequences of ineffective decellularization of biologic scaffolds on the host response. *Biomaterials* **33**, 1771, 2012.
19. Revell, C.M., and Athanasiou, K.A. Success rates and immunologic responses of autogenic, allogenic, and xenogenic treatments to repair articular cartilage defects. *Tissue Eng Part B Rev* **15**, 1, 2008.
20. Adkisson, H.D., Martin, J.A., Amendola, R.L., Milliman, C., Mauch, K.A., Katwal, A.B., Seyedin, M., Amendola, A., Streeter, P.R., and Buckwalter, J.A. The potential of human allogeneic juvenile chondrocytes for restoration of articular cartilage. *Am J Sports Med* **38**, 1324, 2010.
21. Keane, T.J., Swinehart, I.T., and Badylak, S.F. Methods of tissue decellularization used for preparation of biologic scaffolds and in vivo relevance. *Methods* **84**, 25, 2015.
22. Khanlari, A., Detamore, M.S., and Gehrke, S.H. Increasing cross-linking efficiency of methacrylated chondroitin sulfate hydrogels by copolymerization with oligo (ethylene glycol) diacrylates. *Macromolecules* **46**, 9609, 2013.
23. Converse, G., Armstrong, M., Quinn, R., Buse, E., Cromwell, M., Moriarty, S., Lofland, G., Hilbert, S., and Hopkins, R. Effects of cryopreservation, decellularization and novel extracellular matrix conditioning on the quasi-static and time-dependent properties of the pulmonary valve leaflet. *Acta Biomater* **8**, 2722, 2012.
24. Wan, Y.S., Wei-Heng, S., and Ilhan, A.A. Elastic and yield behavior of strongly flocculated colloids. *J Am Ceram Soc* **82**, 616, 2004.
25. Livak, K.J., and Schmittgen, T.D. Analysis of relative gene expression data using real-time quantitative PCR and the $2^{-\Delta\Delta CT}$ method. *Methods* **25**, 402, 2001.
26. Zheng, X., Lu, S., Zhang, W., Liu, S., Huang, J., and Guo, Q. Mesenchymal stem cells on a decellularized cartilage matrix for cartilage tissue engineering. *Biotech Bioprocess Eng* **16**, 593, 2011.
27. Yang, Q., Peng, J., Lu, S., Guo, Q., Zhao, B., Zhang, L., and Wang, A. Evaluation of an extracellular matrix-derived acellular biphasic scaffold/cell construct in the repair of a large articular high-load-bearing osteochondral defect in a canine model. *Chin Med J (Engl)* **124**, 3930, 2011.
28. Moutos, F.T., Estes, B.T., and Guilak, F. Multifunctional hybrid three-dimensionally woven scaffolds for cartilage tissue engineering. *Macromol Biosci* **10**, 1355, 2010.
29. Rowland, C., Lennon, D., Caplan, A., and Guilak, F. The effects of crosslinking of scaffolds engineered from cartilage ECM on the chondrogenic differentiation of MSCs. *Biomaterials* **34**, 5802, 2013.
30. Cheng, N.-C., Estes, B.T., Awad, H.A., and Guilak, F. Chondrogenic differentiation of adipose-derived adult stem

- cells by a porous scaffold derived from native articular cartilage extracellular matrix. *Tissue Eng Part A* **15**, 231, 2008.
31. Gong, J., Sagiv, O., Cai, H., Tsang, S.H., and Del Priore, L.V. Effects of extracellular matrix and neighboring cells on induction of human embryonic stem cells into retinal or retinal pigment epithelial progenitors. *Exp Eye Res* **86**, 957, 2008.
 32. Sellaro, T.L., Ravindra, A.K., Stolz, D.B., and Badylak, S.F. Maintenance of hepatic sinusoidal endothelial cell phenotype in vitro using organ-specific extracellular matrix scaffolds. *Tissue Eng* **13**, 2301, 2007.
 33. Chun, S.Y., Lim, G.J., Kwon, T.G., Kwak, E.K., Kim, B.W., Atala, A., and Yoo, J.J. Identification and characterization of bioactive factors in bladder submucosa matrix. *Biomaterials* **28**, 4251, 2007.
 34. Kanematsu, A., Yamamoto, S., Ozeki, M., Noguchi, T., Kanatani, I., Ogawa, O., and Tabata, Y. Collagenous matrices as release carriers of exogenous growth factors. *Biomaterials* **25**, 4513, 2004.
 35. Gawlitta, D., Benders, K.E., Visser, J., van der Sar, A.S., Kempen, D.H., Theyse, L.F., Malda, J., and Dhert, W.J. Decellularized cartilage-derived matrix as substrate for endochondral bone regeneration. *Tissue Eng Part A* **21**, 694, 2014.
 36. Armstrong, C., and Mow, V. Variations in the intrinsic mechanical properties of human articular cartilage with age, degeneration, and water content. *J Bone Joint Surg* **64**, 88, 1982.
 37. Little, C.J., Bawolin, N.K., and Chen, X. Mechanical properties of natural cartilage and tissue-engineered constructs. *Tissue Eng Part B Rev* **17**, 213, 2011.
 38. Mansour, J.M. Biomechanics of cartilage. In: Oatis CA, ed. *Kinesiology: The Mechanics and Pathomechanics of Human Movement*. Baltimore, MD: Lippincott Williams & Wilkins, 2003, pp. 1992–1996.
 39. Huang, C.-Y., Stankiewicz, A., Ateshian, G.A., and Mow, V.C. Anisotropy, inhomogeneity, and tension–compression nonlinearity of human glenohumeral cartilage in finite deformation. *J Biomech* **38**, 799, 2005.
 40. Schuurman, W., Levett, P.A., Pot, M.W., van Weeren, P.R., Dhert, W.J., Hutmacher, D.W., Melchels, F.P., Klein, T.J., and Malda, J. Gelatin-methacrylamide hydrogels as potential biomaterials for fabrication of tissue-engineered cartilage constructs. *Macromol Biosci* **13**, 551, 2013.
 41. Sridharan, B., Sharma, B., and Detamore, M.S. A road map to commercialization of cartilage therapy in the United States of America. *Tissue Eng Part B Rev* **22**, 15, 2015.
 42. DeKosky, B., Dormer, N., Ingavle, G., Roatch, C., Lomakin, J., Detamore, M., and Gehrke, S. Hierarchically designed agarose and poly(ethylene glycol) interpenetrating network hydrogels for cartilage tissue engineering. *Tissue Eng Part C Methods* **16**, 1533, 2010.
 43. Ingavle, G.C., Dormer, N.H., Gehrke, S.H., and Detamore, M.S. Using chondroitin sulfate to improve the viability and biosynthesis of chondrocytes encapsulated in interpenetrating network (IPN) hydrogels of agarose and poly (ethylene glycol) diacrylate. *J Mater Sci Mater Med* **23**, 157, 2012.
 44. Ingavle, G.C., Frei, A.W., Gehrke, S.H., and Detamore, M.S. Incorporation of aggrecan in interpenetrating network hydrogels to improve cellular performance for cartilage tissue engineering. *Tissue Eng Part A* **19**, 1349, 2013.
 45. Ingavle, G.C., Gehrke, S.H., and Detamore, M.S. The bioactivity of agarose–PEGDA interpenetrating network hydrogels with covalently immobilized RGD peptides and physically entrapped aggrecan. *Biomaterials* **35**, 3558, 2014.
 46. Rennerfeldt, D.A., Renth, A.N., Talata, Z., Gehrke, S.H., and Detamore, M.S. Tuning mechanical performance of poly (ethylene glycol) and agarose interpenetrating network hydrogels for cartilage tissue engineering. *Biomaterials* **34**, 8241, 2013.

Address correspondence to:

Michael S. Detamore, PhD

Department of Chemical and Petroleum Engineering

University of Kansas

4163 Learned Hall

1530 W. 15th Street

Lawrence, KS 66045

E-mail: detamore@ku.edu

Received: December 6, 2015

Accepted: March 21, 2016

Online Publication Date: April 1, 2016